NGU REPORT 2024.029

Exploratory assessment of mineral and organic soil geochemical data from the Møre and Romsdal county: targeting geochemical anomalies

GEOLOGY FOR SOCIETY

SINCE 1858

GEOLOGICAL SURVEY OF NORWAY

- NGU -

NGU REPORT 2024.029

Exploratory assessment of mineral and organic soil geochemical data from the Møre and Romsdal county: targeting geochemical anomalies

GEOLOGICAL SURVEY OF NORWAY
- NGU -

NGU REPORT

Geology for society

Geological Survey of Norway
P.O. Box 6315 Torgarden
NO-7491 Trondheim, Norway
Tel. +47 73 90 40 00

Report no.: 2024.029
ISSN: 0800-3416 (print)
ISSN:2387-3515 (digital)
Grading: Åpen rapport

Title: Exploratory assessment of mineral and organic soil geochemical data from the Møre and Romsdal county: targeting geochemical anomalies
Authors: Pedro Acosta-Góngora, Agnes Raaness, Aziz Nasuti
Client: Møre and Romsdal county
County: Møre and Romsdal
Municipality:

Map-sheet name (M=1:250.000):
Map-sheet name (M=1:50.000):
Deposit name and grid-reference:
Numbers of pages: 31
Price (NOK):

Map enclosures:
Fieldwork carried out: 2021 - 2022
Date of report: 01/12/2024
Project no.: 400600
Person responsible: Siw Taftø
Keywords:

Summary: An exploratory study on C- and O-horizon samples from a low-density regional survey (1 sample per 36 km2) was carried out in the Møre and Romsdal county. Principal component and cluster analyses were implemented to identify samples signaling potential Cu-Zn-Pb, and Fe-Ti-V base metal anomalies. Clustering of the samples (Q-mode) and variables (R-mode) permitted to construct several maps that were used as indicators to identify geochemical anomalies. To complement the multivariate analysis, a percentile-based filtering of the dataset was further used to identify areas with high Fe-V-Ti values. Results from both methods were then contrasted against airborne magnetics. Anomalous samples contained within 4 areas of interest were then selected based on the convergence of two or more anomaly indicators and its coincidence with areas having moderate to high magnetic anomalies. However, further assessment of the magnetic map and the known base metal occurrences show that often, there is not a consistent spatial correlation between the latter and magnetic anomalies.

The biggest limitation of this study is the coarse sampling scale of the geochemical survey compared to the much smaller size of lithological units that host or can potentially host base metal mineralization (e.g., mafic, and ultramafic intrusions are as small as 0.04 km2). Despite the later, this work can be used as first order criterium to identify zones suitable for future and more detailed geoscientific surveys (e.g., geochemistry, geophysics, bedrock, and structural mapping).

Table of contents

1. INTRODUCTION

The Geological Survey of Norway (NGU) is currently undertaken a 6 x 6 km grid nation-wide geochemical mapping program (GMP), which has nearly covered two thirds of the country (northern to mid-Norway; Reimann et al. 2011; Finne et al. 2014; Finne and Eggen, 2015; Flem et al., 2020; Flem et a., 2021; Flem et al. 2022; Acosta-Góngora et al., 2024a, b). In general, the GMP collects soil (C-horizon) samples, but in some counties like Trøndelag and Hedmark, organic soil (O-horizon) samples have been simultaneously taken at each sample location. The Møre and Romsdal county has been the latest county covered by the GMP, where both, C- and O-horizon samples were taken. Despite its low-density design (1 sample per 36 km^2), the GMP (or portions of it) may contain relevant information that can help to identify potential areas of economic interest.

The Møre and Romsdal county is host to several, but for the most part, small base metal occurrences (mineral showings, advanced exploration projects and past-producing mines) with different genetic affinities, that span from e.g., Cu-Zn hydrothermal deposits associated with volcanogenic massive sulfide (e.g. Vassdal deposit) to Fe-Ti(±V±Mn) magmatic deposits (e.g. Maurdal deposit) (Fig. 1). Regardless of their origin, these occurrences are comprised by distinct mineralization/alteration assemblages and hosted by different rock types, which results in contrasting geochemical signatures commonly preserved soil samples. In many instances, such signatures can often be de-coupled by the implementation of several geostatistical approaches. Unsupervised machine-learning (USML) is commonly used for identifying and understanding patterns in geochemical data (e.g., stream sediments, soil and rock). These patterns indicate different geological/geochemical processes that can be undetected by evaluation of single-element concentrations. Among the most popular pattern recognition methods are principal component analysis (PCA) (e.g., Parsa et al. 2017; Montsion et al. 2019), factor analysis (FA) (e.g., Liu et al. 2014) and cluster analysis (CA) (e.g., Templ et al. 2008; Geranian and Carranza 2022; Acosta-Góngora et al. 2022).

In this study, we carry out an exploratory assessment of the Møre and Romsdal county datasets (soil and humus) by implementing PCA and CA to identify potential zones of interest suitable for future and more detailed mineral exploration studies. In addition, we elaborate on the limitations of USML when analyzing low-density geochemical surveys comprising organic and mineral soil material.

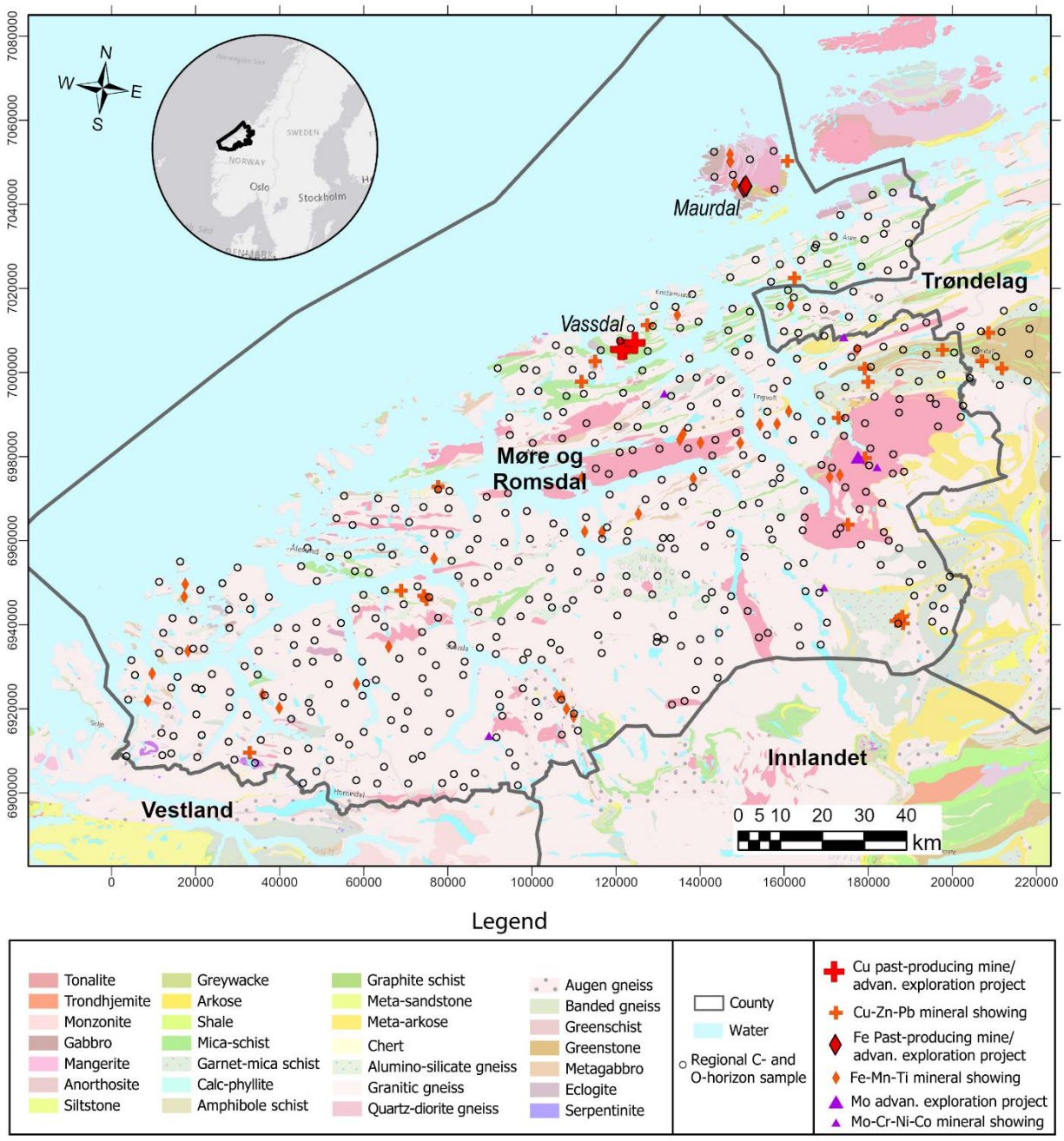

Figure 1. *Bedrock geology of the survey area. The Møre and Romsdal county is marked with a black line and the location of the C- and O-horizon samples are represented by the open black circles. Bedrock units are from NGUs 1:1 350 000 scale bedrock map of Norway (Geological Survey of Norway, 2021).*

2. DESCRIPTION OF THE SURVEY AREA

2.1 Regional geology

Møre and Romsdal County is mainly characterized by granitic gneisses comprised within an area known as the Western Gneiss Region (WGR). These granitic gneisses were formed between 1700 and 1600 Ma and derived from igneous sources. Subsequently, they were strongly deformed and metamorphosed during the Caledonian Orogeny (ca. 420–390 Ma).

During Caledonian continent-continent collision with Laurentia (Greenland), the WGR was subducted to mantle depths, locally in excess of 100 km, and this is marked by the widespread occurrence of high-pressure eclogite lenses, particularly along the western parts that were subjected to the highest pressures (Cuthbert et al., 2000; Hacker and Gans, 2005). The subduction also resulted in fragments of this mantle getting stuck to the downgoing continental slab –found as lenses of olivine-rich mantle peridotite.

During the Caledonian Orogeny, the WGR was overthrust by nappes, which comprise of schists, amphibolites and marbles and continued deformation led to in-folding of the nappes into the gneissic substrate (Terry et al., 2000; Tucker et al., 2004).

The various rocks therefore represent diverse mineral resources, including marble (allochthonous nappes) and olivine (mantle peridotite fragments). Historically, mining for Fe and Ti was undertaken from mafic rocks associated with the gneisses. Figure 1 shows the bedrock map of Møre and Romsdal, with adjacent areas, based on the NGU bedrock map of Norway with scale 1:1 350 000 (Geological Survey of Norway, 2021).

2.2 Mineral deposits

Well-known mineral resources in Møre and Romsdal county registered in the NGU mineral resource databases (https://geo.ngu.no/kart/mineralressurser_mobil/) include metallic ores such as iron-titanium (e.g., the Raudsand deposit), minor copper and chromium deposits and several occurrences of iron, molybdenum, lead and iron sulphides.

Other resource types include industrial minerals such as olivine, calcium carbonate marble, garnets and minor occurrences of mica, feldspar and quartz. Olivine has been exploited since 1948 for construction, metallurgy, filtration and abrasives. Marble was important as construction materials in the 19th and 20th centuries and calcium carbonate marble is still exploited for several industrial purposes and agricultural use.

Some of these deposits and occurrences may contain critical minerals and metals. Iron-titanium deposits are known to have vanadium-bearing magnetite, while some of the old copper mines and occurrences at Averøy are known to be rich in cobalt and scandium. Olivine may also become important for magnesium metal production if the technology for this if commercialized. (Gautneb et al. 2024).

3.METHODS

3.1 Geochemical sampling and analysis

Mineral and organic soil survey sampling locations were selected in the field, preferably close to the centre of a 6 x 6 km grid, yielding a sampling density of 1 sample/ per 36 km^2 (Fig. 1). Mineral soil samples were collected from a single pit in the C-horizon, primarily comprised by till but also weathered rock. Organic soil samples (upper 3 cm of organic material; O-horizon) were pooled from a minimum of 5 subsamples within an area of 100-200 m^2 centred at the corresponding soil sample location. After drying at temperatures below 30 °C, samples were

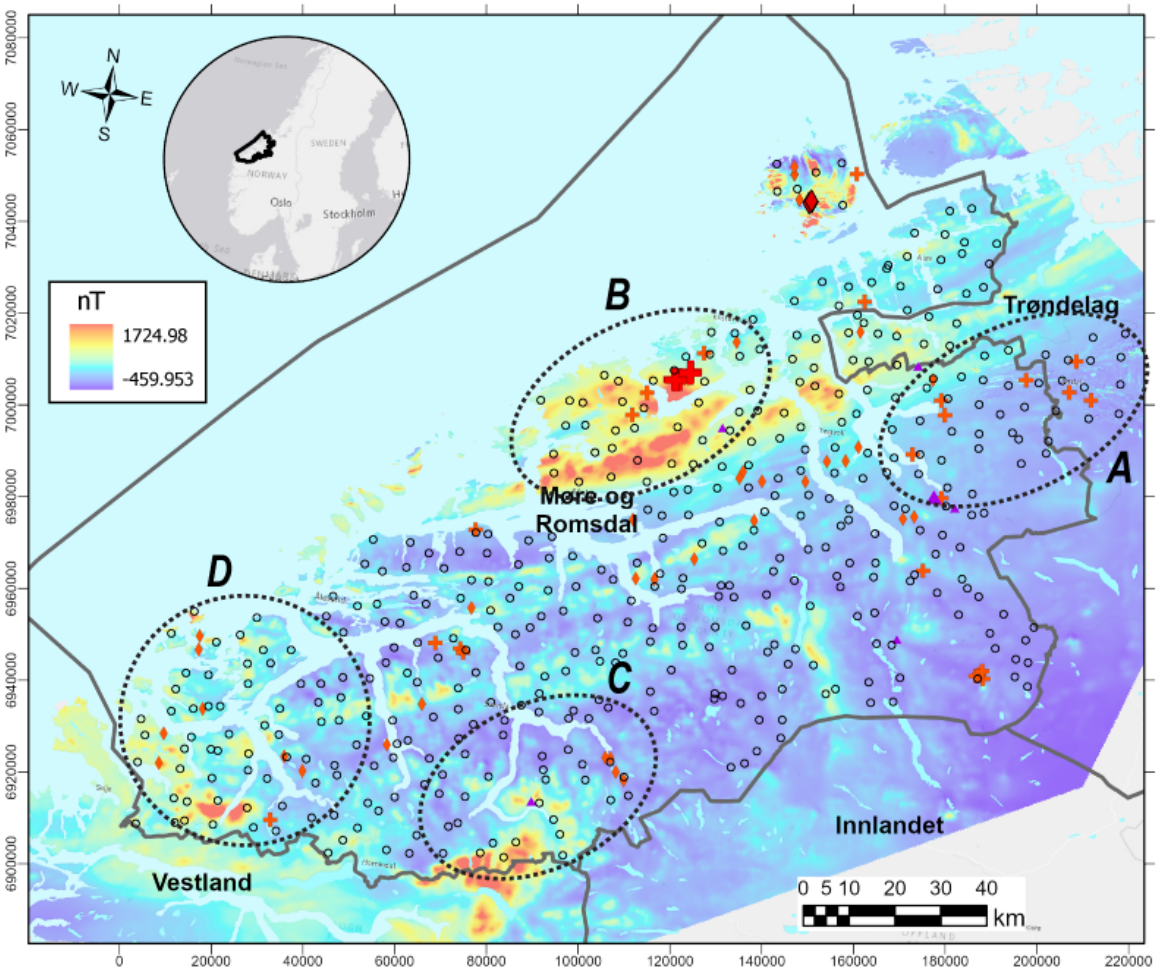

Figure 2. Magnetic anomaly map (compiled by Nasuti et al. 2015). The Møre and Romsdal county outlined with a black line. Location of zones of interest A-D, which are later discussed in figures 9 and 10. Symbology for mineral occurrence types is the same as in Figure 1.

sieved through nylon mesh to less than 2 mm. Detailed procedures on the C- and O-horizon sampling can be found in Eggen et al. (2017), Flem et al. (2020), Flem et al. (2021). Before sending the samples for analytical quantification, these were randomized following procedures described in Eggen et al. (2019). In this study, the C- and O-horizons are also referred as "soil", "humus", respectively.

The samples used for the regional study were analyzed in Bureau Veritas Mineras Laboratories (former ACME labs, Canada). The C- and O-horizon samples were digested in Aqua Regia and analysed by ICP-MS for 53 elements (Al, As, Au ,B ,Ba, Be, Bi, Ca, Cd, Ce, Co, Cr, Cs, Cu, Fe, Ga ,Ge, Hf, Hg, In, K, La, Li, Mg, Mn, Mo, Na, Nd, Ni, P, Pb, Pd, Pt, Rb, Re, S, Sb, Sc, Se, Sn, Sr, Ta, Te, Th, Ti, Tl, U, V, W, Y, Zn, Zr). The two datasets can be found in https://geo.ngu.no/kart/geokjemi_mobil/ along with their QC reports (Acosta-Góngora et al., 2024a, b).

3.2 Airborne magnetic data

Airborne magnetic data available in the study areas was acquired and compiled by the Geological Survey of Norway (NGU) and can be downloaded www.ngu.no (Fig. 2). Detailed information regarding the acquisition and processing of the regional survey data can be found in Nasuti et al. (2015). Surveys were flown with a helicopter/plane at 250-1000m m line spacing and sensor height of 60-200m above ground for the EM bird/magnetometer. The data was grided at 250 m x 250 m resolution Magnetic data was used to compliment the geostatistical analysis. In the Møre and Romsdal county, base metal occurrences are commonly hosted by mafic and ultramafic rocks. This rocks often contain magnetic minerals such as magnetite and pyrrhotite, which create a magnetic contrast with the surrounding lithologies. Thus, areas with higher magnetic anomaly values are then regarded as more prospective.

3.3 Treatment of geochemical data

A total of 430 samples were used for this study. For all elements, analyses below detection limit were converted into “NA” expressions (not available). Due to the compositional nature of the data, and to avoid “the closure problem”, these are scaled by using additive (alr)-, centered (clr) (Aitchison, 1982; Thió-Henestrosa and Martín-Fernández, 2005), and/or isometric- (ilr) (Egozcue et al., 2003) log-ratio transformations prior to multivariate analysis. Log-ratio transformation requires complete datasets, so only elements with less than 10% missing values (“NA” expressions) were used for further analysis. The remaining missing values were input using the k-nearest neighbours’ method (impKNNa function; Hron et al., 2010) from the R package robCompositions (Templ et al., 2011). In total, only 36 (Mo, Cu, Pb, Zn, Ag, Ni, Co, Mn, Fe, Th, U, Sr, V, Ca, P, La, Cr, Mg, Ba, Ti, Al, Na, K, Sc, Se,Tl, Ga, Cs, Nb, Rb, Sn, Zr, Y, Ce, Be, Li) and 40 (Mo, Cu, Pb, Zn, Ag, Ni, Co, Mn, Fe, U, Sr, Cd, Sb, Bi, Ca, P, La, Cr, Mg, Ba, Ti, B, Al, Na, K, Sc, S, Hg, Se, Ga, Cs, Ge, Hf, Nb, Rb, Sn, Ta, Zr, Y, Ce, Li) elements (out of 53) were used for multivariate analysis of soil and humus datasets, respectively.

3.4 Principal component analysis

Principal components analysis (PCA) is a multivariate statistical technique used to decrease the number of dimensions (i.e., elements) within a given dataset, and re-project the data in two-dimensions (i.e., biplots) such that correlations and anti-correlations of elements can be identified. Robust PCA was performed using the R package robCompositions (Filzmoser et al., 2009; Templ et al., 2011). This variation of PCA first scales the compositional data using an ilr transformation, then performs PCA, and finally, back-transforms the resulting loadings and scores into the clr space where compositional biplots can be shown (Filzmoser et al., 2009).

3.5 Cluster analysis

Clustering is an unsupervised-machine learning approach that groups objects into a number of classes or clusters in such a way that objects in one cluster are very similar and objects in different clusters are quite distinct (Gan et al., 2007). Clustering is performed by using a similarity criterion that can be distance between samples (e.g., Euclidean, Manhattan, Minkowski, Mahalanobis) or similarity/dissimilarity coefficients (e.g., cosine, correlation, Canberra, Bray Curtis) (Cha, 2007; Gan et al., 2007; Shirkhorshidi et al. 2015). Clustering can be performed in two modes, R- and Q-modes. The first mode refers to clustering of the variables (i.e., elements) whereas the second one refers to clustering of the respondents (i.e., samples). Because the purpose of this study is to determine and outline base metal-related geochemical anomalies of interest, the number of clusters used for each clustering iteration was set at three. These clusters represent samples belonging to background population (i.e., samples with low concentrations), possible anomaly population (i.e., samples with moderate concentrations), and probable anomaly population (i.e., samples with high concentration).

3.5.1 Agglomerative Hierarchical Clustering

This clustering method considers initially each sample as a distinct cluster and then, at subsequent steps of an iteration process, clusters with stronger similarity to each other are combined iteratively until only one cluster is left, containing all observations (Templ et al. 2008; Geranian and Carranza 2021). Different from other clustering methods, hierarchical clustering does not need to specify the number of clusters, and as such, it is not sensitive to outlier data (Han et al., 2011; Kuchaki Rafsanjani et al., 2012; Popat and Emmanuel, 2014). Therefore, the user can choose the number of clusters as a final condition. In this study, AHC clustering was done using the “agnes” function of the “cluster” R package (Maechler, 2023). Euclidean

distance was used as the distance metric input and the ward method (Ward 1963) as the linking criteria, because it merges clusters with a minimum information loss criteria based on sums of squares (Templ et al. 2008).

3.5.2 Fuzzy C-means clustering

Different from hard clustering algorithms (i.e. classification of each data point set to a unique class or cluster), Fuzzy clustering associates each data point in the data set with every cluster using a membership function (Gan et al. 2007). For each observation (i.e., sample) a membership coefficient (0 to 1) to all clusters is calculated, suggesting how strong the observation is associated with each cluster (0 no association, 1 high association; Gan et al. 2007). Fuzzy clustering results can be shown as classes or in terms of individual cluster membership coefficient. When shown as classes, the sample is classified as part of the cluster for which the highest membership coefficient is achieved. Conversely, as membership coefficients are often transformed to an interval between 0 and 1, these values can be plotted using a continuous color scale.

Fuzzy c-means (FCM) algorithm was carried in this study, and clusters are formed based on the distance between samples and cluster centroids and the membership coefficient was calculated within an interval that ranges from 0 to 1 (Bezdek, 1981). The FCM clustering was performed using the "fcm" function of the "ppclust" R package (Cebeci, 2018). For this clustering approach, the principal component scores were used as the input data, and the distance metric input was the correlation coefficient.

3.6 Multivariate analysis workflow

The workflow implemented for the multivariate analysis is shown in Figure 3. The C- and O-horizon datasets were assessed equally, but only relevant results obtained for each media are presented in this report (Fig. 3). The data was first explored by carrying out robust principal component analysis in which biplots displaying the variable loadings and PC scores were used to assess correlations and anti-correlations of several elements (Figs. 3). Then, Q-mode clustering was carried out using the Fuzzy-C means algorithm by imputing the first seven PCs, which represent close to 80% of the data variability (Clustering approach 1). A knowledge-

driven evaluation was done to identify the cluster signaling base metal mineralization(s) (i.e., probable anomaly clusters).

R-mode clustering (Clustering approach 2; Fig. 3) was then implemented using AHC on the variables, where the data was scaled using the clr-transformation prior to clustering. The AHC clustering is visually displayed as a dendrogram (Figs. 3). In this "tree-like" structure (Figs.4), elements contained in the same "branch" are more correlated than those occurring at e.g., at opposite ends of the "tree" (i.e., different branches). Based on the dendrogram, different subsets of elements (i.e., matrices) were identified and interpreted in terms of lithological units and/or mineralization types (Figs. 4A, B). Matrices relevant to this study (i.e., containing base metals of interest) were chosen based on expert knowledge, and then these were individually clustered

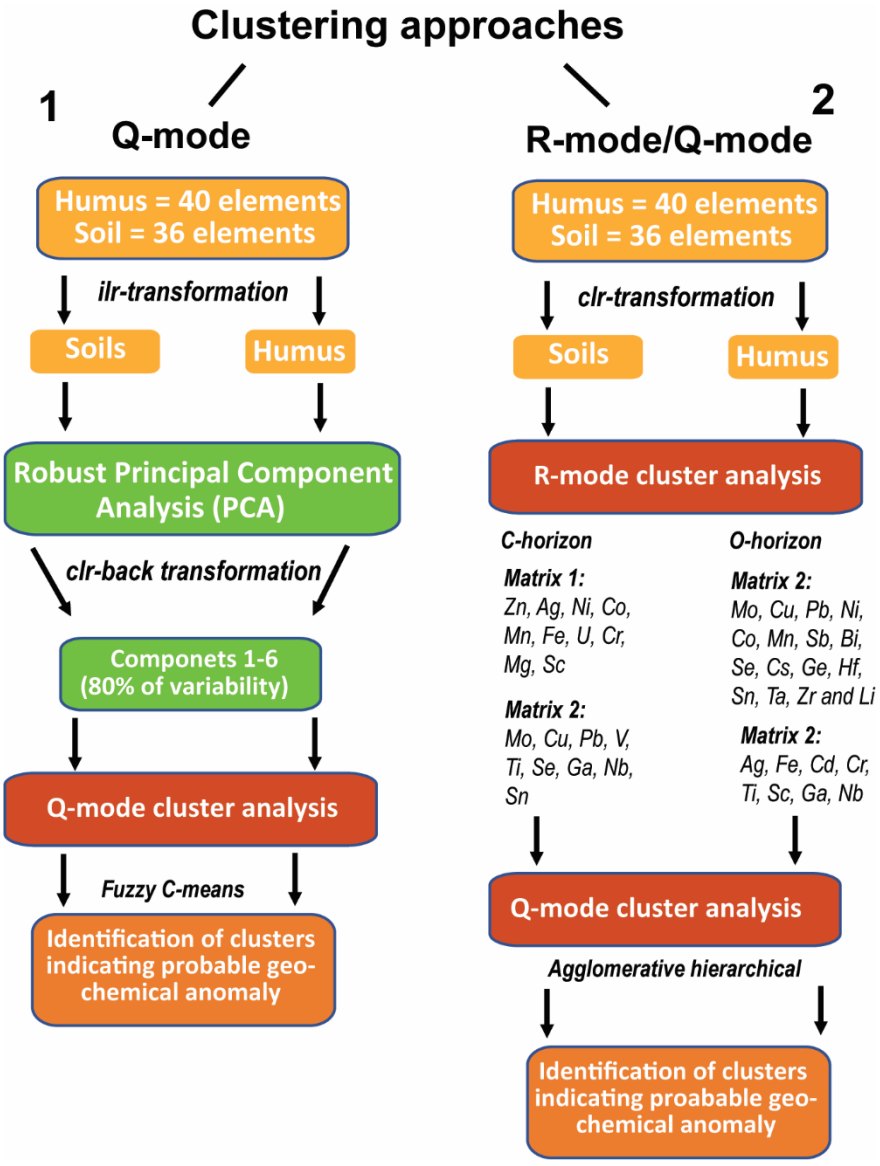

***Figure 3**. Multivariate analysis workflow. Clustering approaches 1 and 2 are shown in separate "branches" of the workflow.*

in Q-mode using the AHC method. In the same way, probable anomaly clusters were identified for each matrix.

3.7 Percentile-based anomaly identification

A quantile-based geochemical anomaly identification was implemented to complement the multivariate analysis. The focus of this approach was set on Fe-V-Ti anomalies which are associated with mafic to ultramafic intrusions. These less conspicuous lithologies are under-represented within the survey (i.e., few samples are collected on C- and O-horizons lying on top of these units), and thus, they can be overlooked by dimension reduction (PCA) and clustering (CA) methods.

The C- and O-horizon datasets were first scaled separately by applying a center-log transformation. Then, base metals of interest were selected (Fe, V, Ti) and their log-ratios normalized to values between 0 (proxy to lowest concentration) and 1 (proxy to highest concentration). Finally, samples with values equal to, or above the 75^{th} percentile (or 4^{th} quantile) for the three elements, Fe-Ti-V were filtered and interpreted as indicative of a geochemical anomaly.

4. RESULTS AND DISCUSSION

4.1 Nature of the materials analyzed

In Norway, most mineral soils (C-horizon) are developed on till material. The term “till” refers to surficial sediments deposited by glaciers that have been exposed to weathering since the last deglaciation (8000 to 12000 years). Till sediments are produced by glacial erosion, entrainment, transportation, and depositional processes (i.e., glacial ice movement) where bedrock is the main source (McClenaghan et al. 2022). On the other hand, organic soil, commonly referred to as “humus”, is not genetically linked to soil formation, whether the former is developed in-situ (e.g., mechanical, and chemical weathering) or has a transported nature like that formed on till.

Humus (O-horizon) corresponds with dark, organic material that forms in soil when plant and animal matter decays. The geochemical composition of humus depends on various complex-biochemical mechanisms, including element transfer from the mineral soil to plants by root uptake and the return of these elements to the humus layer by leaching or decaying plant material ('vascular pump') (Steinnes and Njåstad, 1995). However, biochemical reactions leading to O-horizon formation tend to significantly enrich the O-horizon in some elements,

such as e.g., Mn, Cd and Pb relative to C-horizon (Broster et al. 2009). This preferential partitioning of selected elements disturbs the original geochemical signature of the source material (i.e., C- horizon) by "blurring" correlations and anticorrelation of elements originally partitioned in mineral phases. Meaning that, while multivariate analysis of till sediments geochemistry (i.e., detritus derived from mechanically eroded bedrock) can be used as a proxy

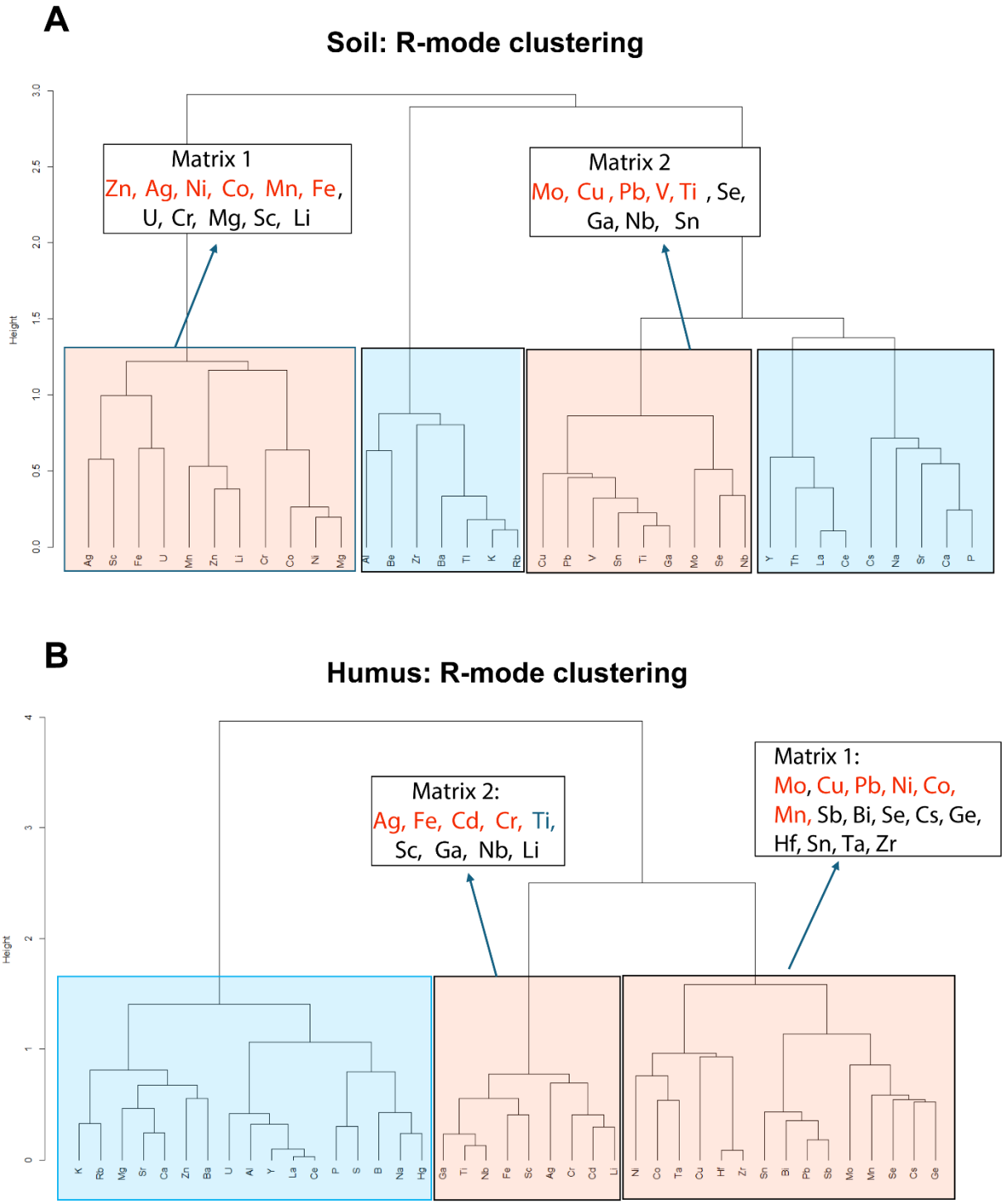

Figure 4. *R-mode clustering for soil (C-horizon) and humus (O-horizon). Elements comprising the matrices used for subsequent Q-mode clustering are highlighted.*

to geological processes, humus could be less efficient to do so due to its biochemical overprint. This is why, univariate analysis of humus data (e.g., individually assessing the spatial distribution of elements of interest) can yield more straightforward results when it comes to bedrock mapping and mineral exploration (e.g., Reimann et al. 2015).

In the following description, the results of the multivariate analysis are under the scope of geological and/or geochemical processes. In cases where results are noisy or less understandable, the description is limited to notice the geographical occurrence of principal component scores and clusters.

4.2 Principal component analysis

4.2.1 Soil (C-horizon)

The first seven principal components (PC1 to PC7) correspond to the linear combinations of selected elements that account for 80% of the variability in the dataset. Here, we will only discuss the first three (57%; PC1=28%, PC2=17%, PC3=12%; Figs. 5A, B). The PC1 axis yields highly negative loadings for Ba, K, and P and highly positive loadings principally for Mo, and to a lesser extent for Se, U, Nb, and Ag. Principal component axis 2 (PC2) yields high negative loadings for Zr, Ca, Na and P and positive loadings for Rb, Ba, K and Ag whereas PC3 is dominated by large negative Ag loadings and positive loadings for Zr, Cr, Se, and Ni.

In general, principal component axes 1 (PC1) and 3 (PC3) can roughly differentiate mafic rocks (amphibolite, greenstone, and intrusions) and mica-rich schists from felsic gneisses. (Fig. 6A, E) However, in the northeastern portion of the county, granitic and mica-rich units, different from the gneiss, are also highlighted by these components. High loadings of principal components 1 and 3 are mainly found in the northern portion of the county where mica-schists and greenstone are more conspicuous (Figs. 1; 6A, E). Conversely, in the southern portion of the county, lower scores are mainly constrained in areas where felsic gneisses are dominant (Figs. 1; 6A, E). However, some intermediate to high values of PC1 and PC3 scores seen in southern Møre and Romsdal could be associated with the occurrence of several small mafic and ultramafic intrusions (<1km^2 diameter) or slivers of mica-schists present in this area. Molybdenum, Ni, and Se are chalcophile elements which are normally contained in sulfide phases, moreover, nickel can also be partitioned along with Cr in ferromagnesian minerals crystallized in mafic rocks (e.g., olivine). Sulfide-rich Cu-Zn base metal deposits are well known to occur to the north in equivalent metasedimentary and mafic volcanic rocks from the

neighboring the Trøndelag county (e.g., Løkken-Røros districts). While PC1 and PC3 can be roughly linked with lithological units, results from PC2 (high Na loading; Fig 6C) appear to be disturbed by environmental processes. In Figure 6C, it is noticeable that larger PC2 scores are found further in land relative to lower PC2 scores, suggesting the influence of Na-rich marine aerosols. These can affect the distribution of all other elements due to a continuous competition for binding sites in the soil (on clays as well as on organic substances in addition to direct chemical reactions with anions like Cl, Reimann et al. 2015).

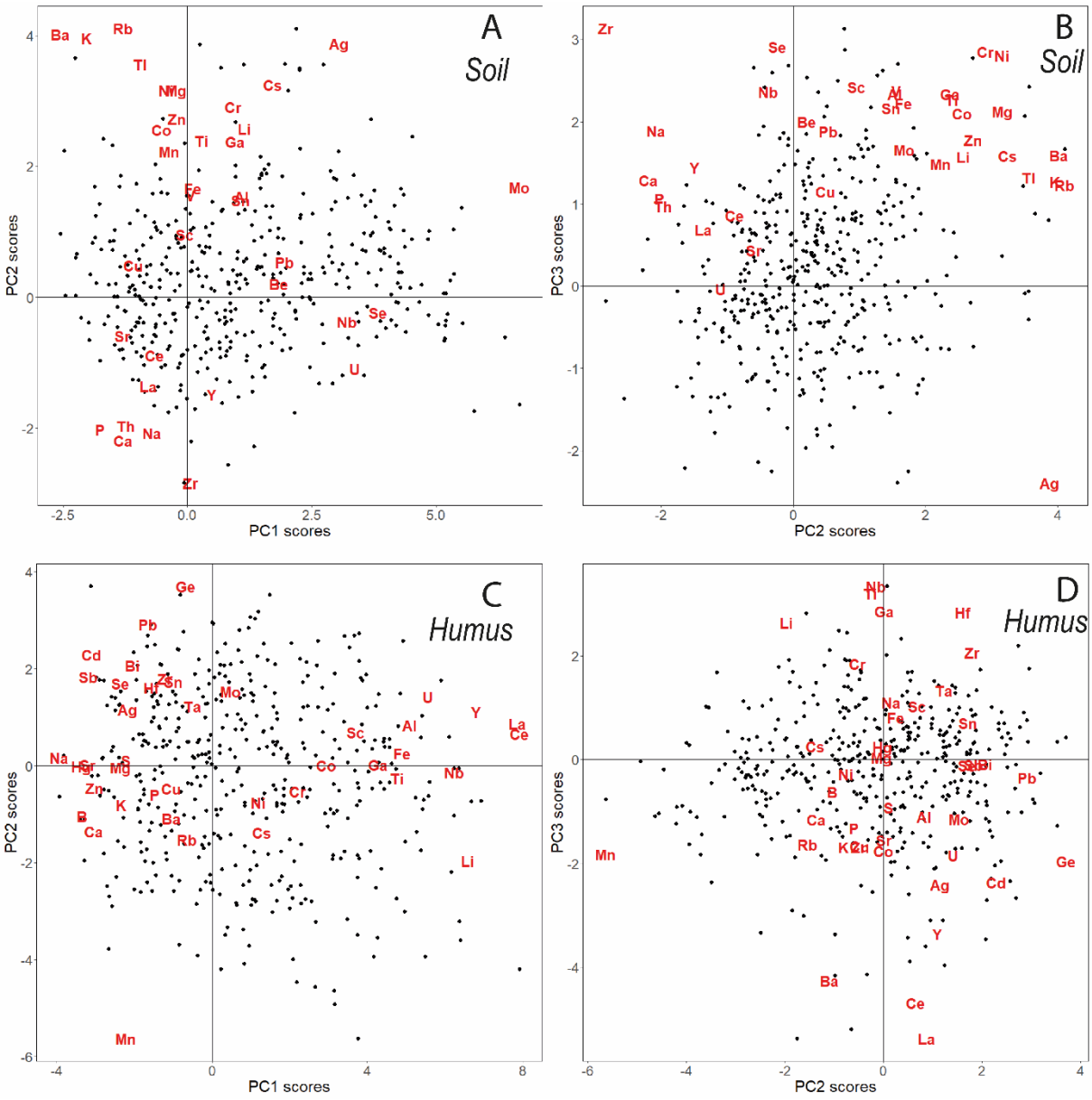

***Figure 5**. Principal component analysis. Biplots showing sample scores and element loadings for principal component axes 1, 2 and 3.*

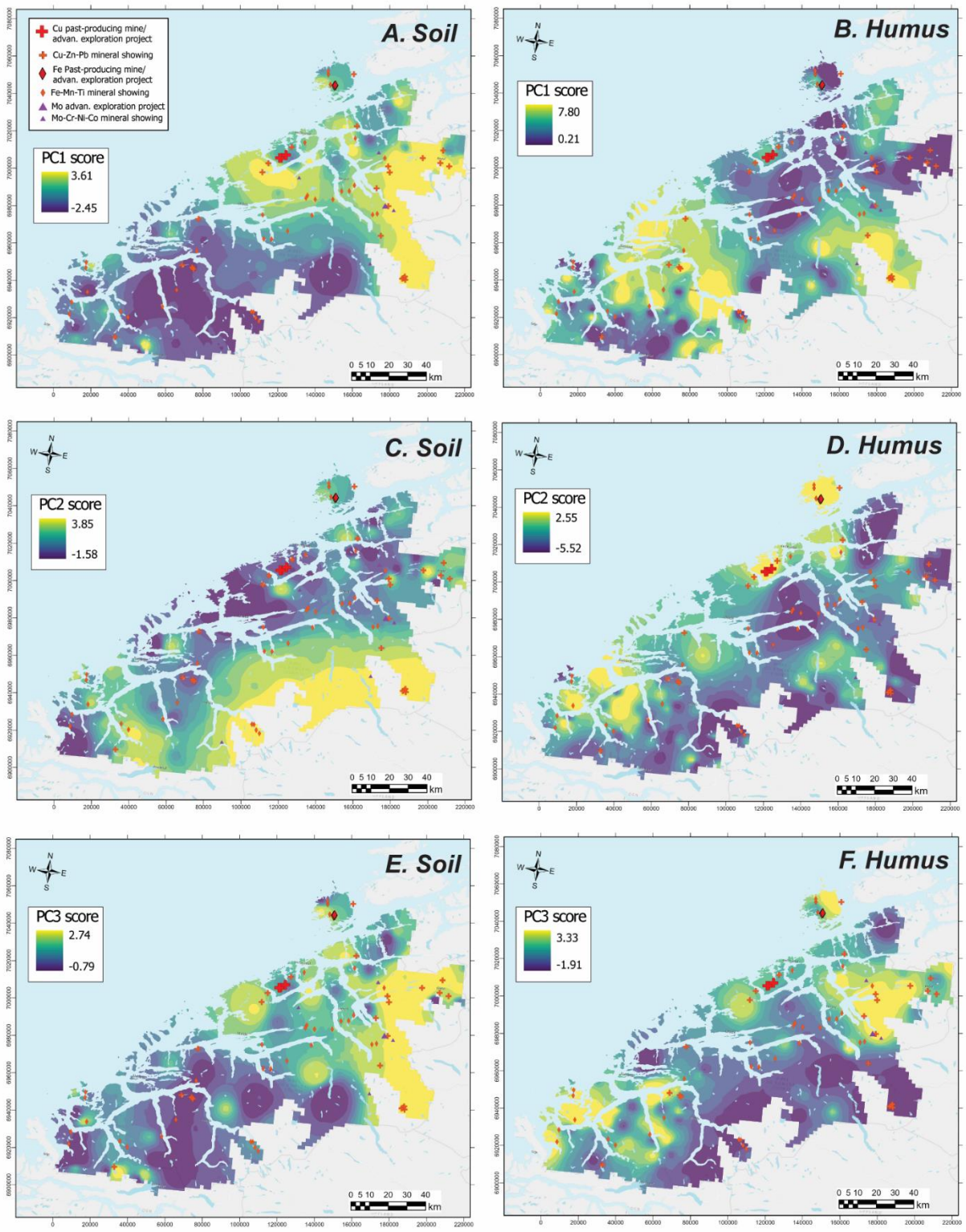

***Figure 6**. Inverse distance interpolation maps of principal component scores 1 to 3 for soil and humus datasets. The interpolations are constrained to the area covered by the survey, and not by the extent of the county.*

4.2.2 Humus (O-horizon)

Like soil, the humus data shows that the first seven principal components (PC1 to PC7) explain 80% of the variability in the dataset, with the first three components comprising 31%, 21% and 7% of it (Figs. 5C, D). The PC1 axis yields highly negative loadings for Na, Hg, and B and

highly positive loadings principally for La, Ce, Y, Li and Nb. The PC2 axis achieves negative loadings principally for Mn and less for Li and Rb and positive loadings for Ge, Pb and Cd. The PC3 axis achieves negative loadings for Ba, Y, Ce and La, and positive loadings for Nb, Ti, Ga and Hf.

Roughly, low PC1 scores characterize areas where metasedimentary rocks are more dominant, at least in northern Møre and Romsdal (Figs. 1; 6B). Notably, larger PC2 score values are somewhat associated with areas containing multiple intermediate to ultramafic intrusions (Figs. 1; 6D). However, this is less obvious in Figure 1 because the intrusions are often smaller than 1 km^2. We then encouraged the reader to review the online version of the bedrock map. Principal component 3 (Fig. 6F) scores are less constrained to specific lithologies but indicate some spatial correlation (higher scores) with slivers of greenstone and associated mica-sedimentary rocks in the northern portion of the county. Despite the "noisy" results, most likely derived from a combination of environmental and biochemical processes, some spatial correlation between bedrock and O-horizon geochemistry can be inferred from the regional data.

4.3 Cluster analysis

4.3.1 Soil (C-horizon)

Results from the Q-mode clustering indicate that the cluster representing probable anomaly comprises 22% of the dataset (Figs. 7A, C). This cluster has higher concentrations of Co, Ni, Cr and Ti, relative to the other two, but comparable concentrations of Cu and Zn relative to the probable anomaly cluster (Figs. 7E). In general, samples comprising the probable anomaly cluster have a good spatial association with Cu-Zn-Pb sulfide-rich mineralization, and less often with Fe-Mn-Ti (e.g., Smøla island) and Fe(±Cr±Ni±Co±V±Mo±W) occurrences (Figs. 7A, C). In terms of its lithological association, the prospective samples are mainly contained within slivers of greenstone, amphibolite and mica-schists. In cases where these samples are contained in larger felsic gneiss units, it is likely that this is either due to un-mapped strips of the greenstone-amphibolite-mica schist assemblage or that the area occupied by these rocks is too small to be displayed at the current mapping scale. Given the soft-clustering nature of the Fuzzy C-means approach, it is possible to identify samples with higher membership values (i.e., probability in % of being classified as probable anomaly), which can further help to refine the identification of prospective areas.

The clustering of the variables (R-mode clustering) yielded four matrices or clusters (Fig. 4A). However, only two of these were considered for further Q-mode clustering because of their

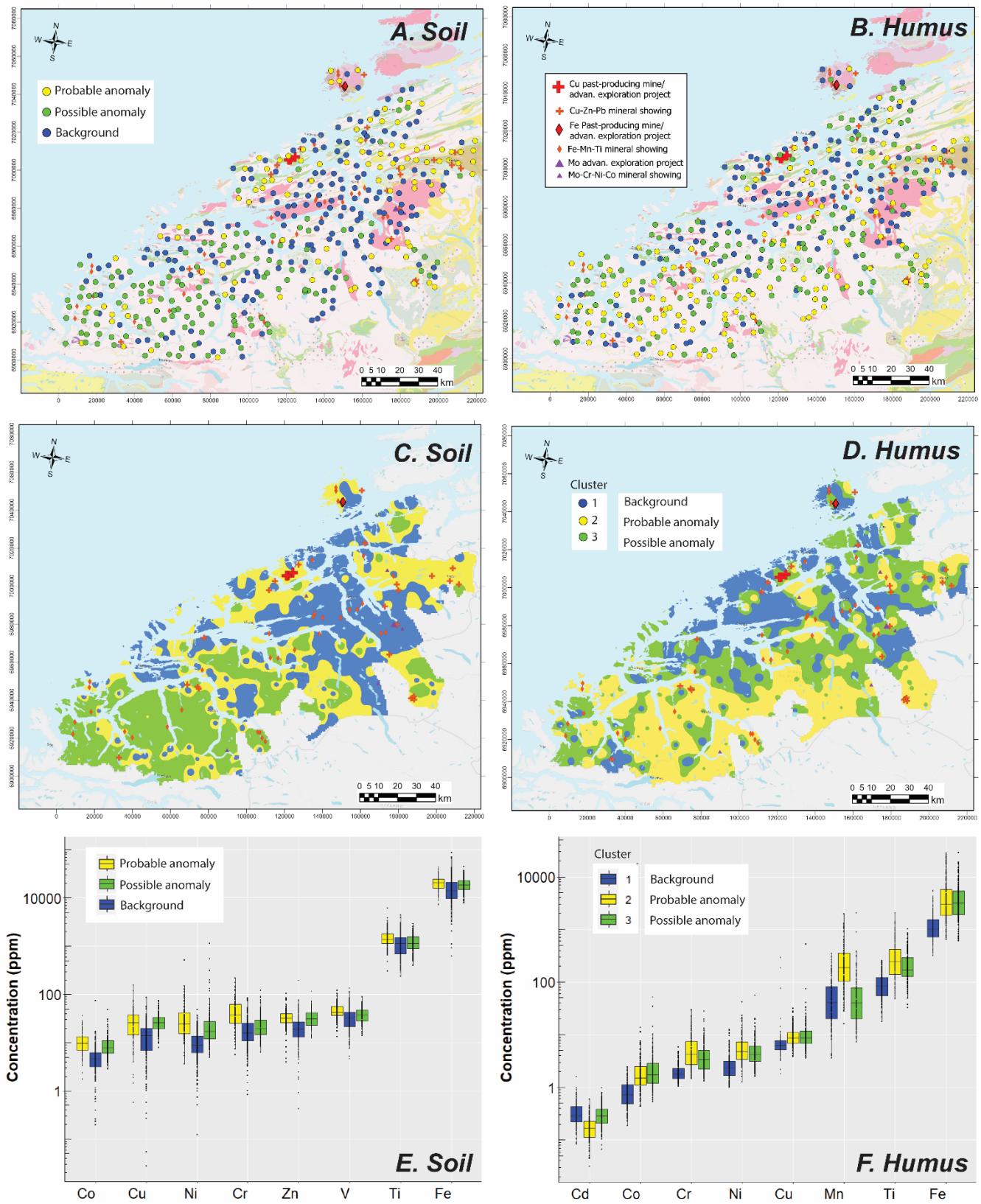

***Figure 7**.Q-mode cluster analysis on C- and O-horizon datasets. In A and B are shown the samples classified per cluster type. In C and D are shown IDW maps for the cluster types, and E and F the box-whiskers plots showing base metal concentrations for each cluster.*

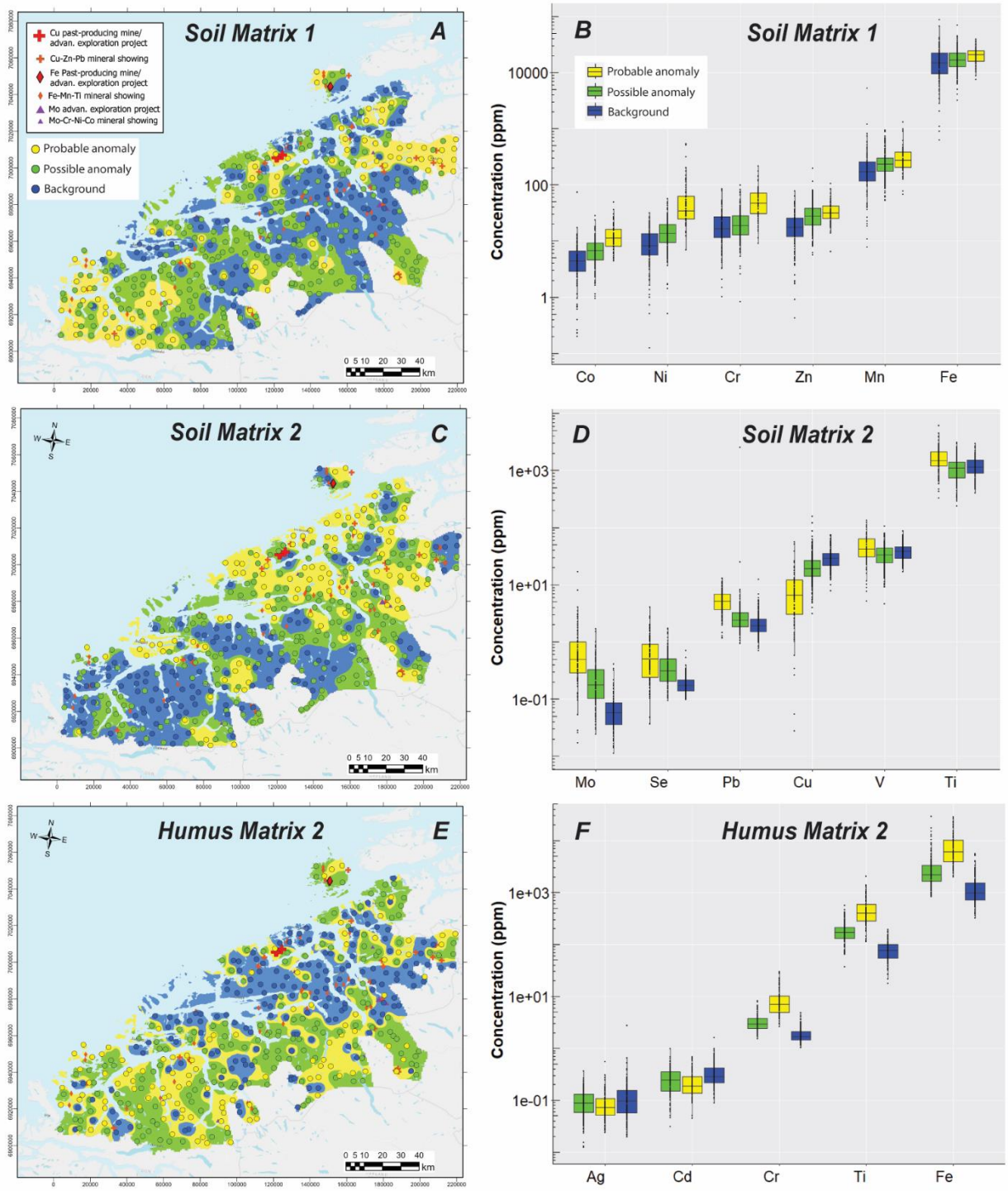

Figure 8. *R-mode clustering results for the soil (C-horizon) and humus (O-horizon) samples. In A and C are shown C-horizon samples classified after clustering and B and D show base metal concentrations as boxplots. In E and F are shown the matrix 2 of the O-horizon cluster analysis and respective box-plots displaying the concentration distribution.*

association with base metals of interest. The first matrix includes Zn, Ag, Ni, Co, Mn, Fe, U, Cr, Mg, Sc and Li, whereas the second one is comprised by Mo, Cu, Pb, V, Ti, Se, Ga, Nb, Sn.

The AHC results for matrix one indicates that the probable anomaly cluster accounts for 18% of the dataset and achieves the highest Co, Ni, Cr, Zn and Mn values of all three clusters (Fig. 8A, B). A closer look to the location of these samples indicates that several are either contained

within mafic lithologies (greenstone, amphibolite, gabbro, anorthosite peridotite) or located relatively nearby them (< 6 km). As a result, the anomalous samples can be roughly separated in two groups occupying the northern and southern portions of the county. The northern portion is dominated by greenstone and amphibolite, whereas the south contains several small mafic to ultramafic intrusions. For matrix two, the AHC results show that samples suggesting a probable geochemical anomaly account for 23% of the dataset and are enriched in Mo, Se, Pb, V and Ti (Figs. 8C, D). Like matrix one, samples from the probable anomaly cluster can be geographically located over mica-schist, and less often over amphibolite, but there is less obvious association among this cluster, specific rock types and mineral occurrences.

4.3.2 Humus (O-horizon)

Results from the Q-mode clustering for the humus dataset are more difficult to interpret (Figs.7B, D, F), and as such, a clearly prospective cluster (i.e., probable anomaly) cannot be easily identified. In the following description, the percentage of the dataset comprised by each cluster is given in parenthesis. Cluster 1 (35%) contains the lowest base metal values, except for Cd (Figs. 7B, D, F), and thus, this can be interpreted as the closest to background. Cluster 2 (31%) accounts for the highest Cr, Ni, Mn and Ti concentrations, whereas cluster 3 (34%) achieves the highest Co concentrations (not shown) but has comparable amounts of Cu and Fe relative to cluster 2 (Figs. 7B, D, F). Although, the clusters hold no obvious spatial correlation between specific lithologies and/or base metal occurrences, it is noted that cluster 1 occurs predominantly in the mid and northern portions of the county, perhaps indicating some influence from with the greenstone belt packages. On the other hand, cluster 2 occurs mostly in the middle and southern portions of the county, possibly indicating some input from mafic and ultramafic intrusions, given its high base metal content.

Three matrices were defined by R-mode clustering (Fig. 4B), but only two of these were considered for further Q-mode clustering based on their association with base metals. The first matrix includes Mo, Cu, Pb, Ni, Co, Mn, Sb, Bi, Se, Cs, Ge, Hf, Sn, Ta, Zr and Li, whereas the second one is comprised by Ag, Fe, Cd, Cr, Ti, Sc, Ga, and Nb.

For matrix 1 (not shown), the cluster selected as probable anomaly accounts for 25% of the dataset and it achieves the highest concentrations for most base metals (Co, Ni, Cu, and Mn). In matrix 2, the probable anomaly cluster (25% of the dataset) yielded the largest concentrations for Cr, Ti and Fe (Figs. 8E, F). Geographically, both clusters are mostly constrained to the middle and southern parts of the county (Fig. 8E).

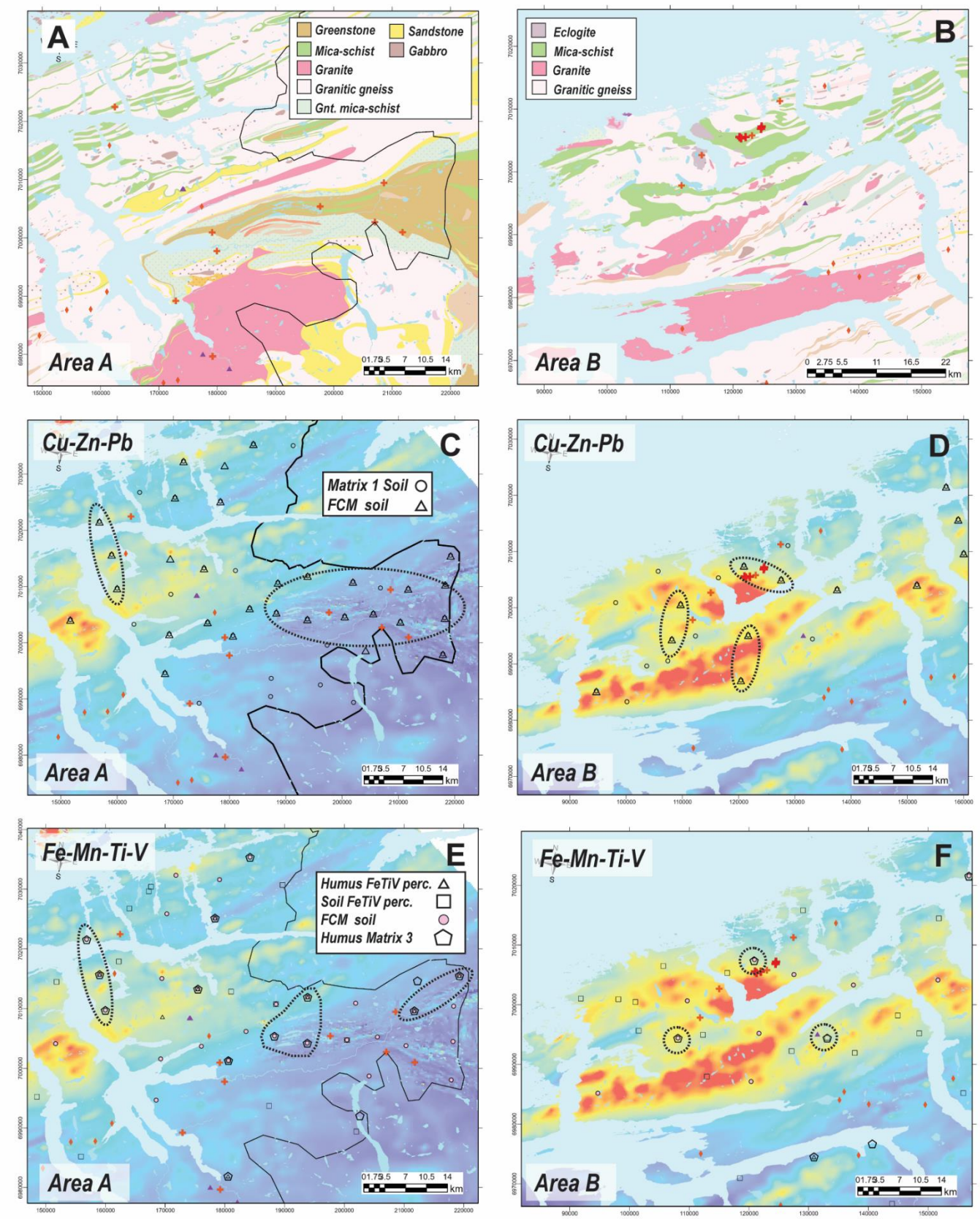

Figure 9. *Prospective **Areas A** and **B** as shown in Figure 2. Zones or samples of interest, where 2 or more base metal indicators coincide and fall on top of moderate to large magnetic anomalies are further highlighted by the dashed lines. In A, C and E, and B, D and F are shown the geology, and zones/samples of interest for Cu-Zn-Pb and Fe-Ti-Mn-V mineralization types in **Areas A** and **B**, respectively. In figures A and B, the legend for the dominant lithologies is provided. The rest of the rock unit labels are as in Figure 1. Mineral occurrences symbology as given in previous figures.*

4.4 Limitations of the multivariate approach

The multivariate approach shows that several under-represented geochemical processes (e.g., different types of mineralization) account for the large variability of the O- and C-horizon datasets. Meaning that, e.g., less dominant mineralized/altered rocks or lithologies present in the area are under-sampled in the survey and thus, cannot be easily de-coupled from the dominant geochemical signatures (i.e., lithologies). This is further inferred from the fact that it takes up to seven components to achieve 80% of the data variability.

The other constraining factor is the scale of the survey, which combined with the scattered nature and small size of mafic, ultramafic and metasedimentary rocks (especially in the south) in this county, limits greatly our ability to recognized well-defined base metal anomalies. For example, Fe-V-Ti occurrences are often hosted by < 1km^2 mafic and ultramafic intrusions, which are almost an order of magnitude smaller than survey's resolution. Despite the latter, it is possible to identify many areas in the Møre and Romsdal county where several geochemical anomaly vectors tested in this study converge, and thus, these can be taken as first order criteria to allocate resources for future and more detailed surveys.

5. PROSPECTIVE AREAS

In this study we have carried out an exploratory analysis of the C- and O-horizons geochemical data by testing multiple geochemical proxies or indicators for base metal mineralization (CA, PCA and percentile-based filtering). Each of these proxies can be used as individual vectors for mineral exploration. Thus, it is up to the reader to assess the information provided here and decide whether a particular vector(s) is more relevant than other(s) given the geological framework of the Møre and Romsdal county. In the following description we put emphasis on 4 areas (A to D) where samples having 2 or more geochemical anomaly vectors coincide with high magnetic anomalies indicating potential Cu-Zn-Pb and/or Fe-Mn-Ti-V mineralization (Figs. 2, 9, 10). In Figure 2 are shown the general locations of these prospective areas. Zones of interest within these areas are further highlighted in figures 9 and 10. Often, anomalous samples indicating areas with potential for both mineralization types (Cu-Zn-Pb and Fe-Mn-Ti-V) are equivalent. This suggests that at the scale of the study, it is not possible to fully distinguish between different types of mafic lithologies (e.g., anorthosite-gabbro versus greenstone-amphibolite).

Area A is located in northern Møre and Romsdal and it is dominated by slivers of greenstone belts, amphibolite, metgabbro and mica-rich metasedimentary rocks (Fig. 9A, B). Here, multivariate analysis and percentile-filtering indicate potential for the two types of base metal

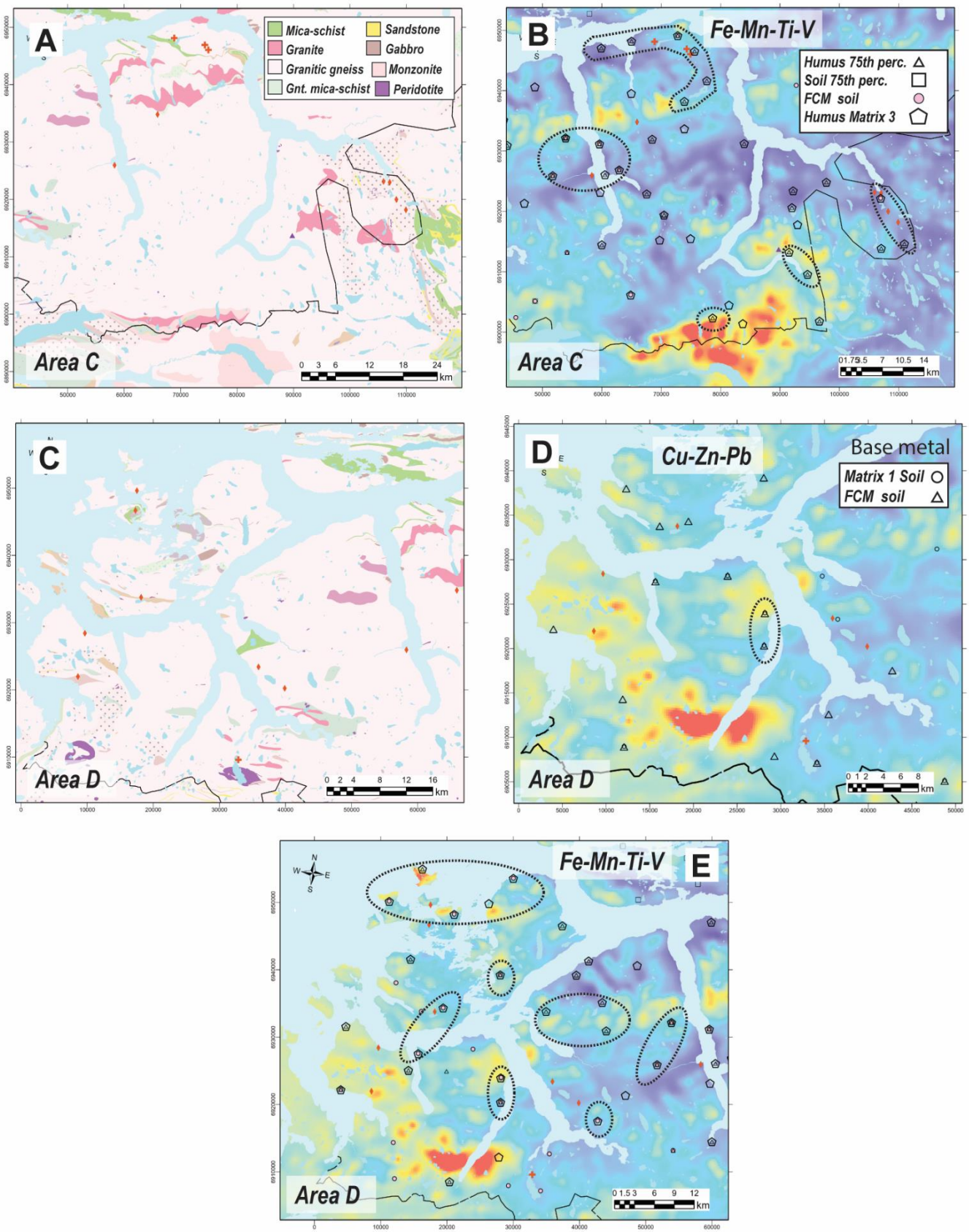

Figure 9. *Prospective **Areas C** and **D** as shown in Figure 2. Zones or samples of interest, where 2 or more base metal indicators coincide and fall on top of moderate to large magnetic anomalies are further highlighted by the dashed lines. In A and B, and C to E are shown zones/samples of interest for Cu-Zn-Pb and Fe-Ti-Mn-V mineralization types in **Areas C** and **D**, respectively. In figures A and C, the legend for the dominant lithologies is provided. The rest of the rock unit labels are as in Figure 1. Mineral occurrences symbology as given in previous figures.*

mineralization. Especial attention should be given to samples with three indicators for the Fe-

Ti-V type mineralization (Fig. 9 E).

Area B occurs in the western portion of the county, and it is characterized by a several samples that lie within a large magnetic high, where several past-producing Cu-Zn mines occur (Figs. 9B, D, F). The geology of the area is characterized by the presence of mica-rich metasediments (host to the past-producing mines), several gabbroic intrusions, amphibolite and a highly magnetic granite (Fig. 9B). Other minor Fe-Mn-Ti-V-Mn occurrences are emplaced just to the southeast, and they coincide with small and relatively intermediate magnetic values likely indicating the presence of small mafic and ultramafic intrusions. However, only 3 Fe-Ti-V anomalous humus samples are found around some of these (Fig. 9F). In general, these smaller occurrences are not captured by the geochemical survey.

Area C (southern Møre and Romsdal) is dominated by granitic gneiss crosscut by several small (down to 0.04 km^2) ultramafic and mafic intrusions (Fig. 10A). The magnetic anomaly map shows two areas with relatively large magnetic highs located in the north and south of Area C (Fig. 10B). The northern high is associated with the occurrence of roughly E-NE trending metagabbro-granite assemblage with less important slivers of mica-rich metasedimentary rocks. The southern high is associated with the emplacement of monzonite and granite. Samples classified as Fe-Mn-Ti-V anomalous by 2 to 3 indicators were detected close of known Cu-Zn-Pb and Fe-Mn-Ti-V showings (Fig. 10B). A number of these anomalous samples fall either on top of the large magnetic highs or adjacent to moderate magnetic anomalies.

Area D is located west of Area C, and both are geologically comparable as several mafic to ultramafic intrusions and amphibolite occur within the larger granitic gneiss (Fig. 10C). Anomalous O- and C-horizon samples signalling Cu-Zn-Pb and Fe-Mn-Ti-V mineralization occur in some cases close to known Fe-Mn-Ti-V showings. A high magnetic anomaly is recognized in the south and coincides in part with the location of augen gneiss and anorthosite intrusions. However, no base metal occurrence neither anomalous C- or O-horizon samples are located on top of it. Conversely, smaller, and less prominent areas with moderate magnetic highs host some of the anomalous samples. It is also noted that most of the known Fe-Ti-V and Cu-Zn-Pb showings are not linked to the emplacement of magnetic highs, but rather associated intermediate low magnetic susceptibility values (Fig. 10E).

6. SUMMARY

An exploratory data analysis on C- and O-horizon samples from a low-density regional survey (1 sample per 36 km^2) was carried out in the Møre and Romsdal county. Principal component and cluster analyses were implemented to identify samples signalling potential Cu-Zn-Pb, and Fe-Mn-Ti-V base metal anomalies. Clustering was done in Q- and R-modes which allowed to construct several indicators or vectors for geochemical anomaly mapping. To complement the multivariate analysis, a percentile-based filtering of the datasets was further used to identify areas with high Fe-V-Ti values. Both approaches were then contrasted against airborne magnetics. Highly anomalous samples contained within 4 areas of interest were then chosen based on the convergence of multiple anomaly indicators and its coincidence with areas having high magnetic susceptibility values. However, further assessment of the magnetic and bedrock maps and the locations of the base metal occurrences show that there is not systematic spatial correlation among them.

As expected, the biggest limitation of this work is the coarse sampling scale of the geochemical survey compared to the much smaller size of lithological units (e.g., mafic, and ultramafic intrusions could be as small as 0.04 km^2) hosting base metal mineralization. Despite the later, this work can be used as first order criterium to identify zones suitable for future and more detailed geoscientific surveys (e.g., geochemistry, geophysics, bedrock, and structural mapping).

ACKNOWLEDGMENTS

We thank the soil sampling team for the fieldwork: Malin Andersson, Rut Eikeland, Tor Erik Finne, Belinda Flem, Ivar Haukdal, Iain Henderson, Sverre Iversen, Ane Bang-Kittelsen, Åse Minde, Agnes Raaness, Hild Sissel Thorsnes, and Guri Venvik.

The staff at geomatics are acknowledged for assistance during the preparation of field map and ArcGIS Collector. In addition, gratitude is express to Sverre Iversen for making field photos available.

REFERENCES

Acosta-Góngora, P., Andersson, M., Finne, T.E., Taftø, S., Venvik, G., 2024a. Organic soil geochemistry in the Møre and Romsdal county. Geological Survey of Norway, Report 2014.001, pp. 97.

Acosta-Góngora, P., Andersson, M., Finne, T.E., Taftø, S., Venvik, G., 2024b. Mineral soil geochemistry in the Møre and Romsdal county. Geological Survey of Norway, Report 2014.002, pp. 95.

Acosta-Góngora, P., Potter, E.G., Lawley, C.J.M., Corriveau, L., Sparkes, G., 2022. Geochemical characterization of the Central Mineral Belt U ± Cu ± Mo ± V mineralization, Labrador, Canada: Application of unsupervised machine-learning for evaluation of IOCG and affiliated mineral potential. Journal of Geochemical Exploration 237:106995. https://doi.org/10.1016/j.gexplo.2022.106995.

Aitchison, J., 1982. The Statistical Analysis of Compositional Data. Chapman and Hall, London. https://doi.org/10.1002/bimj.4710300705.

Broster, B.E., Dickson, M., Parkhill, M.A., 2009. Comparison of humus and till as prospecting material in areas of thick overburden and multiple ice-flow events: An example from northeastern New Brunswick. Journal of Geochemical Exploration 103:115-132.

Bezdek, J.C., 1973. Cluster Validity with Fuzzy Sets. Journal of Cybernetics 3:58-73.

Cebeci, Z., 2019. Comparison of internal validity indices for fuzzy clustering. Journal of Agricultural Informatics 10:1-14. doi:10.17700/jai.2019.10.2.537.

Cha, S. H., 2007. Comprehensive survey on distance/similarity measures between probability density functions. International Journal of Mathematical Models and Methods in Applied Science 1:300-307.

Cuthbert, S.J., Carswell, D.A., Krogh-Ravna, E.J., and Wain, A. 2000. Eclogites and eclogites in the Western Gneiss Region, Norwegian Caledonides. Lithos 52:165-195. https://doi.org/10.1016/S0024-4937(99)00090-0.

Eggen, O.A., Andersson, M., Gasser, D., 2017. Till geochemistry in Oppdal and Rennebu, Sør-Trøndelag county, Norway. Geological Survey of Norway, Report 2017.023, pp. 111

Eggen O.A., Reimann C., Flem B., 2019. Reliability of geochemical analyses: Deja vu all over again. Science of the Total Environment 670:138-148. https://doi.org/10.1016/j.scitotenv.2019.03.185.

Egozcue, J.J., Pawlowsky-Glahn, V., Mateu-Figueras, G. and Barcelo-Vidal, C., 2003. Isometric logratio transformations for compositional data analysis. Mathematical Geology 35:279–300. https://doi.org/10.1023/A:1023818214614.

Finne, T. E., Reimann, C., Eggen, O. A., 2014. Mineral soil geochemistry in Nord-Trøndelag and Fosen. Geological Survey of Norway, Report 2014.047, pp. 91.

Finne, T. E., Eggen, O. A., 2015. Organic soil geochemistry in Nord-Trøndelag and Fosen. Norges geologiske undersøkelse, Serie/Kilde: NGU-rapport 2014.057, pp. 82.

Filzmoser, P., Hron, K., Reimann, C., 2009. Univariate statistical analysis of environmental (compositional) data: Problems and possibilities. Science of Total Environment 407: 6100–6108. https:/doi:j.scitotenv.2009.08.008.

Flem, B., Andersson, M., Finne, T. E., Minde, Å., 2020. Mineral soil geochemistry in southern Trøndelag. Geological Survey of Norway. Report 2020.017, pp. 127.

Flem, B., Acosta-Gongora, P., Andersson, M., Minde, Å, Finne, T. E., 2021. Organic soil geochemistry in southern Trøndelag, QC – report. Geological Survey of Norway. Report 2021.006, pp. 123.

Flem, B., Acosta-Gongora, Finne, T.E., Klug, M., 2022. Mineral soil geochemistry in Hedmark county, QC – report. Geological Survey of Norway, Report 2022.021, pp. 31.

Gan, G., Ma, C., Wu, J., 2007. Data Clustering: Theory, Algorithms, and Applications. ASA-SIAM Series on Statistics and Applied Mathematics, 448 pp. https://doi:10.1137/1.9780898718348.

Gautneb, H., Bjerkgård, T., Sandstad, J.S., 2024. Overview of critical metals and minerals in Norway. Geological Survey of Norway report 2024.023 https://www.ngu.no/upload/Publikasjoner/Rapporter/2024/2024_023.pdf

Geological Survey of Norway, 2021. Bedrock map of Norway 1:1 350 000. https://www.ngu.no/upload/Publikasjoner/Kart/BGNorge_1350_000.pdf

Geranian, H., Carranza, E.J.M., 2022. Mapping of regional-scale multi-element geochemical anomalies using hierarchical clustering Algorithms. Natural Resources Research 31:1841-1865. https://doi.org/10.1007/s11053-021-09879-5.

Hacker, B.R., and Gans, P.B. 2005. Continental collisions and the creation of ultrahigh-pressure terranes: Petrology and thermochronology of nappes in the central Scandinavian Caledonides. Geological Society of America Bulletin 117:117-134.

Han, J., Kamber, M., and Pei, J., 2011. Data mining: Concepts and techniques. 3rd Edition. Morgan Kaufmann, 744 pp.

Hron, K., Templ, M., Filzmoser, P., 2010. Imputation of missing values for compositional data using classical and robust methods. Computer Statistics and Data Analysis 54:3095-3107. https://doi:10.1016/j.csda.2009.11.023.

Kuchaki Rafsanjani, M., Asghari Varzaneh, Z., Emami Chukanlo, N., 2012. A survey of hierarchical clustering algorithms. The Journal of Mathematical and Computer Science 5: 229-240.

Liu, Y., Cheng, Q., Xia, Q., Wang, X., 2014. Multivariate analysis of stream sediment data from Nanling metallogenic belt, South China. Geochemistry: Exploration, Environment, Analysis: 14:331-340. http://dx.doi.org/10.1144/geochem2013-213.

Maechler, M., Rousseeuw, P., Struyf, A., Hubert, M., Hornik, K., 2023. cluster: Cluster Analysis Basics and Extensions. R package version 2.1.6 — For new features, see the 'NEWS' and the 'Changelog' file in the package source), https://CRAN.R-project.org/package=cluster.

McClenaghan, M.B., Spirito, W.A., Day, S.J.A., McCurdy, M. W., McNeil, R.J., Adcock, S.T., 2022. Overview of surficial geochemistry and indicator mineral surveys and case studies from the Geological Survey of Canada's GEM Program. Geochemistry: Exploration, Environment, Analysis 22: geochem2021-070. https://doi.org/10.1144/geochem2021-070

Montsion, R.M., Saumur, B.M., Acosta-Gongora, P., Gadd, M.G., Tschirhart, P., Tschirhart, V., 2019. Knowledge-driven mineral prospectivity modelling in areas with glacial overburden: porphyry Cu exploration in Quesnellia, British Columbia, Canada. Applied Earth Science 128:181-196.

Nasuti, A., Olesen, O., Barnawal, V. and Dumais, M.-A., 2015. Compilation of aeromagnetic data, in COOP Phase 2 - Crustal Onshore-Ofshore Project, pp. 11–24, eds Olesen, O. et al., Geological Survey of Norway, Report 2015.063, pp. 412.

Steinnes, E., and Njåstad, O., 1995. Enrichment of metals in the organic surface layer of natural soil: identification of contributions from different sources. Analyst 120:1479-1483, https://doi.org/10.1039/AN9952001479.

Parsa, M., Maghsoudi, A., Carranza, E.J.M., Yousefi, M. 2017. Enhancement and Mapping of Weak Multivariate Stream Sediment Geochemical Anomalies in Ahar Area, NW Iran. Natural Resources Research 26:443–455.

Popat, S. K., Emmanuel, M., 2014. Review and comparative study of clustering techniques. International Journal of Computer Science and Information Technologies 5:805-812.

Reimann, C., Finne, T. E., Filzmoser, P., 2011. New geochemical data from a collection of till samples from Nordland, Troms and Finnmark. Geological Survey of Norway, Report 2011.045, pp. 152.

Reimann, C., Schilling, J., Roberts, D., Fabian, K., 2015. A regional-scale geochemical survey of soil O and C horizon samples in Nord-Trøndelag, Central Norway: Geology and mineral potential. Applied Geochemistry 61: 192-205. https://doi.org/10.1016/j.apgeochem.2015.05.019

Shirkhorshidi, A. S., Aghabozorgi, S., Wah, T. Y., 2015. A comparison study on similarity and dissimilarity measures in clustering continuous data. PLoS ONE 10: 1-20.

Templ, M., Filzmoser, P., Reimann, C., 2008. Cluster analysis applied to regional geochemical data: Problems and possibilities. Applied Geochemistry, v. 23:2198-2213. https://doi.org/10.1016/j.apgeochem.2008.03.004.

Templ M, Hron K, Filzmoser P., 2011. robCompositions: an R-package for robust statistical analysis of compositional data. John Wiley and Sons. ISBN 978-0-470-71135-4, doi:10.1002/9781119976462.ch25.

Thió-Henestrosa, S., Martín-Fernández, J., 2005. Dealing with compositional data: The freeware CoDaPack. Mathematical Geoscience: 37:773–793. https://doi: 10.1007/s11004-005-7379-3.

Terry, M.P., Robinson, P., Ravna, E.J.K., 2000: Kyanite eclogite thermobarometry and evidence for thrusting of UHP over HP metamorphic rocks, Nordøyane, Western Gneiss Region, Norway. American Mineralogist 85:1637-1650.

Tucker, R.D., Robinson, P., Solli, A., Gee, D.G., Thorsnes, T., Krogh, T.E., Nordgulen, Ø., Bickford, M.E., 2004: Thrusting and extension in the Scandian hinterland, Norway: New U-Pb ages and tectonostratigraphic evidence. American Journal of Science 304:477-532.

Ward, J.H., 1963. Hierarchical Grouping to Optimize an Objective Function. Journal of the American Statistical Association 58:236-244.

GEOLOGICAL
SURVEY OF
NORWAY

· NGU ·

Geological Survey of Norway
PO Box 6315, Sluppen
N-7491 Trondheim, Norway

Visitor address
Leiv Eirikssons vei 39
7040 Trondheim

Tel (+ 47) 73 90 40 00
E-mail ngu@ngu.no
Web www.ngu.no/en-gb/